

Received:
22 January 2019
Revised:
21 March 2019
Accepted:
18 April 2019

Cite as: Yu Liu, Dongqi Yang, Yuanchun Zhao, Yanqiu Yang, Shiwei Wu, Jing Wang, Lixin Xia, Peng Song. Solvent-controlled plasmon-assisted surface catalysis reaction of 4-aminothiophenol dimerizing to p,p'-dimercaptoazobenzene on Ag nanoparticles. *Heliyon* 5 (2019) e01545. doi: 10.1016/j.heliyon.2019.e01545



Solvent-controlled plasmon-assisted surface catalysis reaction of 4-aminothiophenol dimerizing to p,p'-dimercaptoazobenzene on Ag nanoparticles

Yu Liu^a, Dongqi Yang^a, Yuanchun Zhao^a, Yanqiu Yang^a, Shiwei Wu^{a,c}, Jing Wang^a, Lixin Xia^{a,**}, Peng Song^{b,*}

^a College of Chemistry, Liaoning University, Shenyang 110036, China

^b College of Physical, Liaoning University, Shenyang 110036, China

^c Experimental Center of Shenyang Normal University, Shenyang 110034, China

* Corresponding author.

** Corresponding author.

E-mail addresses: lixinxia@lnu.edu.cn (L. Xia), pengsong@lnu.edu.cn (P. Song).

Abstract

A large number of literatures have investigated the selective photocatalytic reaction of 4-aminothiophenol (PATP) to p,p'-dimercaptoazobenzene (DMAB). Most of them mainly study the contribution of substrate, excitation wavelength, exposure time, pH and added cations to plasmon-assisted surface catalytic reactions. However, we mainly study focuses on the effects of solvents on the dimerization of PATP to DMAB under the action of Ag nanoparticles (NPs). In experiments, a variety of diols was selected as solvents for the probe molecule PATP, and power-dependent SERS spectra were obtained at an excitation wavelength of 532 nm. From the laser-dependent SERS spectrum, we found that the characteristic peak enhancement effect of the product DMAB in different solvents is significantly different. That is, different solvents could regulate the rate at which DMAB is produced from PATP. Based on the experimental results, we further

explored how different diol solvents regulate the response of PATP to DMAB. Our conclusion is that the solvent in the system can quickly capture the hot electrons generated by the decay of the plasmon, so that the remaining holes can oxidize PATP to form DMAB. The ability to trap hot electrons is different due to the difference in the position of the functional groups in the solvent, so that the photocatalytic reaction rate of the hole-oxidized PATP is different. The ability to capture electrons varies depending on the position of the functional groups in the solvent, so the oxidation rate of the photocatalytic reaction is also different. This work not only deepens our understanding of the mechanism of hole-driven surface catalysis oxidation reaction, but also provides a convenient method for regulating the rate of catalytic oxidation.

Keywords: Analytical chemistry

1. Introduction

Surface-enhanced Raman scattering (SERS) refers to a phenomenon where the Raman scattering signal of adsorbed molecules is much greater than the normal Raman scattering (NRS) signal due to the enhancement of the electromagnetic field on, or near, the surface of a sample [1, 2]. The SERS may be 10^5 – 10^8 times greater than the NRS [3]. Due to the resonance absorption of surface plasmons, SERS overcomes the shortcomings of the low sensitivity of Raman spectroscopy [4]. And SERS can obtain molecular structure information that is difficult to obtain by NRS [5, 6, 7]. Therefore, this photoinduced catalytic reaction also brings many applications [8]. For example, it is widely applied to research into the surface state of adsorption interfaces, the interface orientation of biological-size molecules, and configuration, conformational and structural analyses [9]. It can effectively analyze the adsorption orientation of a compound at an interface, changes of the adsorption state, and interface information. Moreover, SERS is widely used in medical testing, pesticide analysis, safety inspections, single molecule detection and identification, chemistry, biology, and physics due to its excellent characteristics [10, 11, 12]. At present, the SERS enhancement mechanisms generally recognized by the academic community include physical and chemical enhancement mechanisms. The former mainly result from local electromagnetic field enhancement caused by the surface plasmon resonance of noble metals under photoexcitation. The latter are mainly charge transfer processes caused by mutual chemical interactions between an adsorbate and a reinforcing substrate [13, 14].

SERS is also often used to study the mechanisms and kinetics of surface plasmon-driven/assisted oxidation and reduction reactions [15, 16]. 4-nitrothiophenol (PNTTP) is a typical probe molecule used to investigate the plasmon-driven surface catalytic reduction reactions [17]. The hot electrons generated by plasmon decay not only

provide the required electrons for the reduction reaction, but also reduce the kinetic energy barrier of the reaction [18]. However, PATP is often used as a model to study the mechanisms of plasmon-driven surface catalytic oxidation reactions [19]. Mechanisms of oxidation reactions include two main oxidation processes: 1) the hot electrons generated by the plasmon activate the surrounding oxygen and then oxidize the PATP to DMAB as a catalyst, and 2) holes are generated in the plasmon excitation process to drive the oxidation of target molecules [20, 21]. Later, a large number of studies reported the effects of various enhancement substrates, excitation wavelengths, laser power levels and exposure times on surface plasmon-driven/assisted catalytic oxidation and reduction reactions [22, 23, 24, 25]. Sun et al. also studied the effects of surroundings, substrate, voltage and solution pH on surface plasmon-driven surface catalysis reactions [26, 27, 28, 29]. Zhang et al. also reported the effect of different metal ions on plasmon-driven catalytic redox reactions [30].

In this paper, we focus on the contribution of solvent to the plasmon-assisted surface catalytic oxidation reaction of PATP dimerization into DMAB on Ag nanoparticles (NPs). We dissolved the probe molecule PATP in different diol solvents and then mixed them with a silver sol to collect power-dependent SERS spectra at an excitation wavelength of 532 nm. By comparing the intensities of SERS spectra, we found that different solvents affect the rate at which PATP is oxidized to DMAB. Therefore, we believe that various diol solvents can be used as regulators of the oxidation of PATP into DMAB. Combined with the experimental results of the power-dependent SERS spectra of DMAB, we also confirmed that the effects of different diol solvents on the rate of PATP to DMAB vary widely.

2. Materials and methods

Samples of PATP, AgNO₃ and sodium citrate analytical reagent were purchased from J & K Chemical and used without further treatment or purification. 1,2-propanediol, 1,3-propanediol, 1,2-butanediol, 1,3-butanediol, 1,4-butanediol, 2,3-butanediol, 1,2-pentanediol, and 1,5-pentanediol were purchased from Energy Chemical. All solvents were used without further processing.

There are many methods for synthesizing SERS active substrates. In addition to some common precious metal particles, there are some semiconductors, and metal-semiconductors can be used as SERS active substrates. And these materials have also been experimentally proven not only as SERS active substrates, but also widely used in the environment and energy fields [31, 32]. In this paper, we mainly choose AgNPs as the substrate for experimental research. We prepare AgNPs were prepared by the chemical reduction method previously reported by Lee-Meisel et al [33]. We prepared silver sol mainly by the sodium citrate reduction method: 18 mg of silver nitrate (AgNO₃) was poured into a three-necked round bottom flask and

100 ml of deionized water was added to fully dissolve it. The solution was then heated to a slightly boiling state in an oil bath. Next, 2 ml of 1% aqueous sodium citrate solution was added quickly and stirred vigorously. The solution gradually changed from colorless and transparent to pale yellow, then dark yellow and, finally, a gray-green transparent sol was formed. The mixed solution was kept in a slightly boiling state for about 20 min, then cooled to room temperature and refrigerated for use. Transmission electron microscopy (TEM) images of Ag NPs indicate that their particle size was approximately 40 nm (Fig. 1B).

Characterization. We placed PATP powder on a glass slide for normal Raman measurements. Meanwhile, the solution of PATP and aqueous Ag NPs was introduced into capillary sample cells for SERS measurement. Laser intensity-dependent SERS spectra were collected on a Renishaw inVia confocal Raman system with a $50\times$ (NA = 0.75) objective lens and a laser spot of approximately 1 μm diameter. At a wavelength of 532 nm, the laser's power was varied between 0.0025 mW, 0.25 mW, 0.5 mW, and 2.5 mW, and exposure times of 10 s were used.

3. Results and discussion

We first characterized the morphology and particle size of Ag NPs prepared by sodium citrate reduction by scanning electron microscopy (SEM) and TEM. The SEM images show that the surface morphology of the Ag NPs is uniform and spherical (Fig. 1A). The TEM image shows that the Ag NPs have a particle size of about 40 nm (Fig. 1B).

Before studying the surface catalytic oxidation behavior of PATP in different solutions, we first performed Raman characterization of PATP powder (Fig. 2). This shows an obvious and strongest peak at 1084 cm^{-1} that is attributed to the vibrations of ν_{cc} and ν_{cs} . The Raman peaks at 1590 cm^{-1} and 1176 cm^{-1} are attributed to ν_{CC} vibration and ν_{CH} vibration on the benzene ring, respectively. The Raman peak appearing at 1492 cm^{-1} is attributed to the β_{CH} and ν_{CC} vibration modes. The Raman peak appearing at 1289 cm^{-1} is attributed to the vibration mode of $\nu_{\text{C-N}}$ [34].

Fig. 3 shows the power-dependent SERS spectra of PATP in four solvents: 1,2-butanediol, 1,3-butanediol, 1,4-butanediol, and 2,3-butanediol. It can be clearly seen from Fig. 3 (A-C) that three characteristic Raman peaks corresponding to the product DMAB were present at 1141 , 1389 and 1429 cm^{-1} , even with a laser intensity as small as 0.05%. Further comparisons revealed that the three characteristic peaks had different enhancement effects in three different solvents. However, in Fig. 3D, no significant characteristic peak of DMAB was observed at a laser intensity of 0.05%, and a characteristic peak attributed to $-\text{N}=\text{N}-$ was observed when the laser intensity was increased to 0.5%. At the same time, we noticed that unlike the other three solvents, a new peak appeared at 1330 cm^{-1} , which is attributed to the

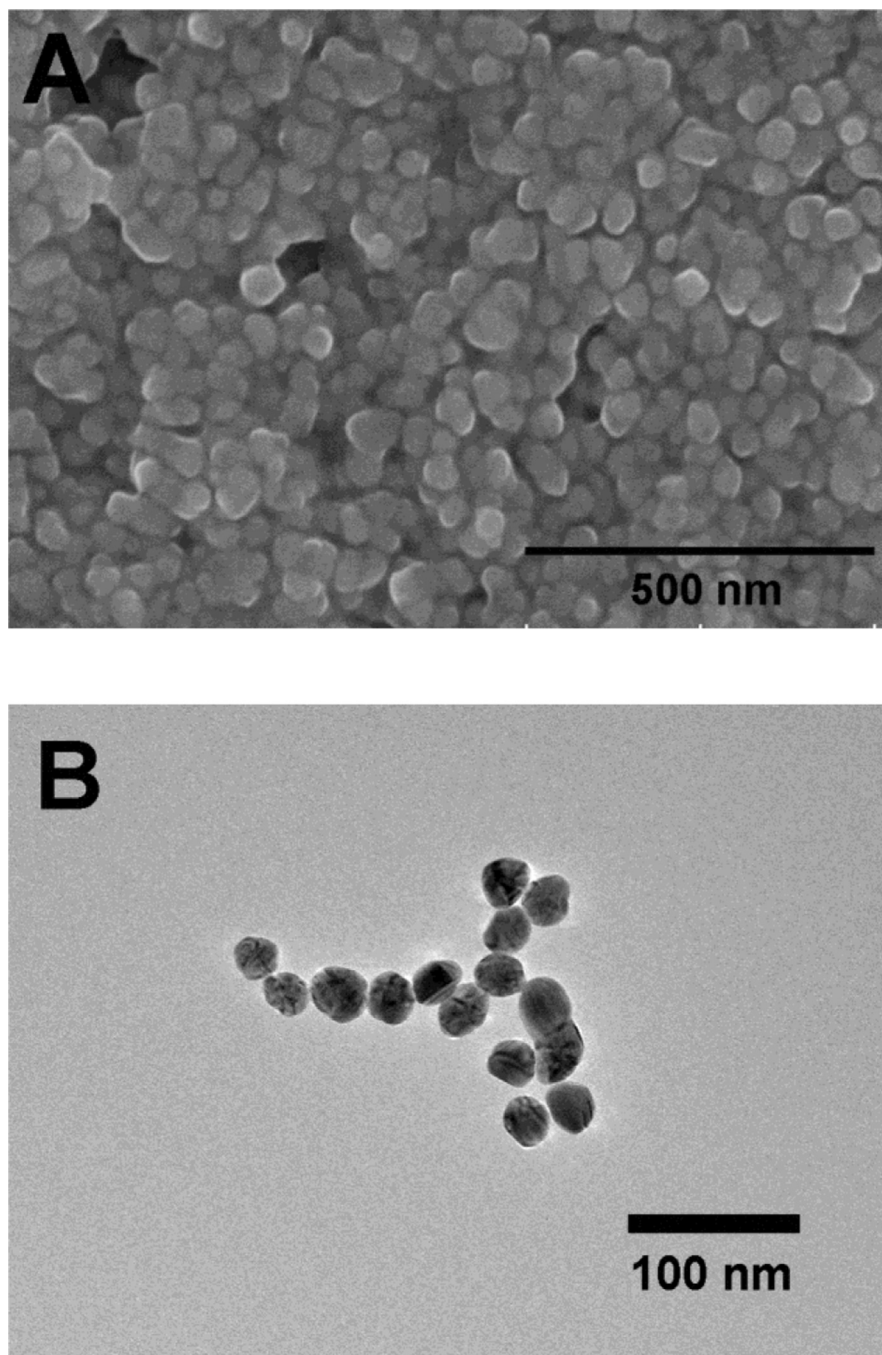


Fig. 1. (A) SEM image of Ag NPs (B) TEM image of Ag NPs.

vibration peak of $-\text{NO}_2$ [35]. That is to say, when PATP is in a 2,3-butanediol solvent, it is not completely oxidized to DMAB, and part of the $-\text{NH}_2$ is oxidized to $-\text{NO}_2$ to form 4-nitrothiophenol (PNTP). The possibility of this phenomenon has also been reported, PATP is difficult to directly oxidize to DMAB under acidic conditions. When the environment in which PATP is located is unfavorable to the

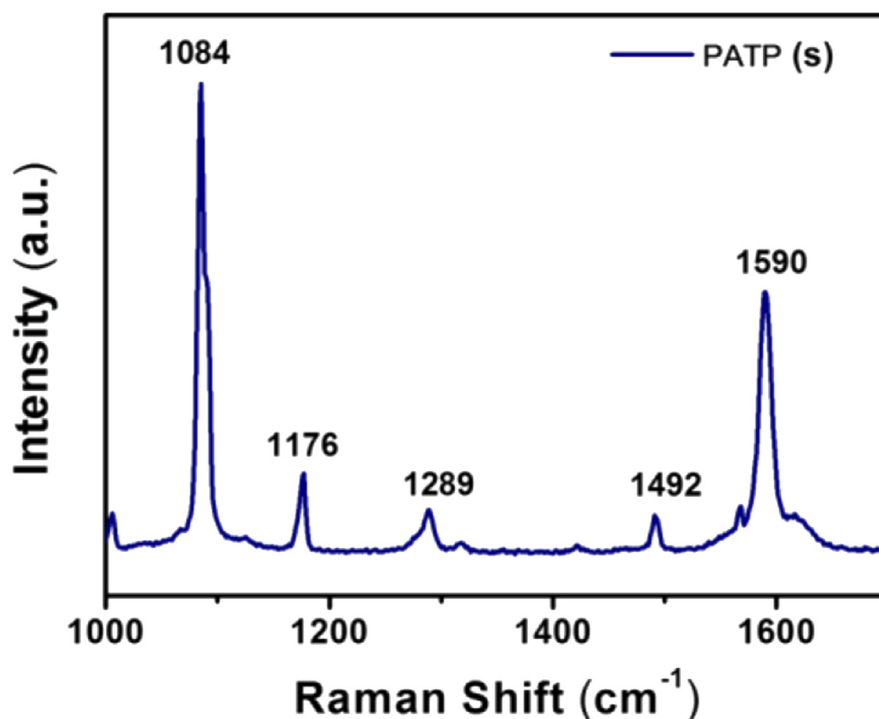


Fig. 2. Normal Raman spectroscopy of PATP powder acquired at a laser wavelength of 532 nm.

deprotonation reaction, it may be oxidized to PNTTP [36, 37, 38]. In summary, from the power-dependent SERS spectra, we found that PATP produced DMAB at the slowest rate in 2,3-butanediol solvent. Based on the above experimental results and discussion, we speculate that PATP dimerizes into DMAB in four different butanediol solvents with different reaction rates. In order to more intuitively observe the effect of solvent on the rate of DMAB generation from PATP, we determined the power-dependent SERS intensities of DMAB, as shown in Fig. 4.

Fig. 4 shows the power-dependent SERS intensity of DMAB in 1,2-butanediol, 1,3-butanediol and 1,4-butanediol. This figure allows direct observation of the effect of three solvents on the enhancement effect. Fig. 4 (A-C) are power dependent SERS intensity plots of DMAB at 1141, 1389 and 1429 cm^{-1} . We can clearly see that the effects of 1,2-butanediol and 1,3-butanediol solvent on the formation rate of DMAB are almost similar with changes of power. However, as the power is increased, the rate of formation of DMAB in the 1,4-butanediol solvent is drastically increased. This graph shows that PATP oxidizes to DMAB at different rates in the three solvents and works best in 1,4-butanediol. Thus, after our structural analysis of the four butanediol solvents, We believe that the difference in the position of substitution of hydroxyl groups on the carbon chain will affect the rate of formation of DMAB. A schematic diagram of the reaction processes whereby DMAB is formed from PATP in the some solvents is shown in Fig. 5.

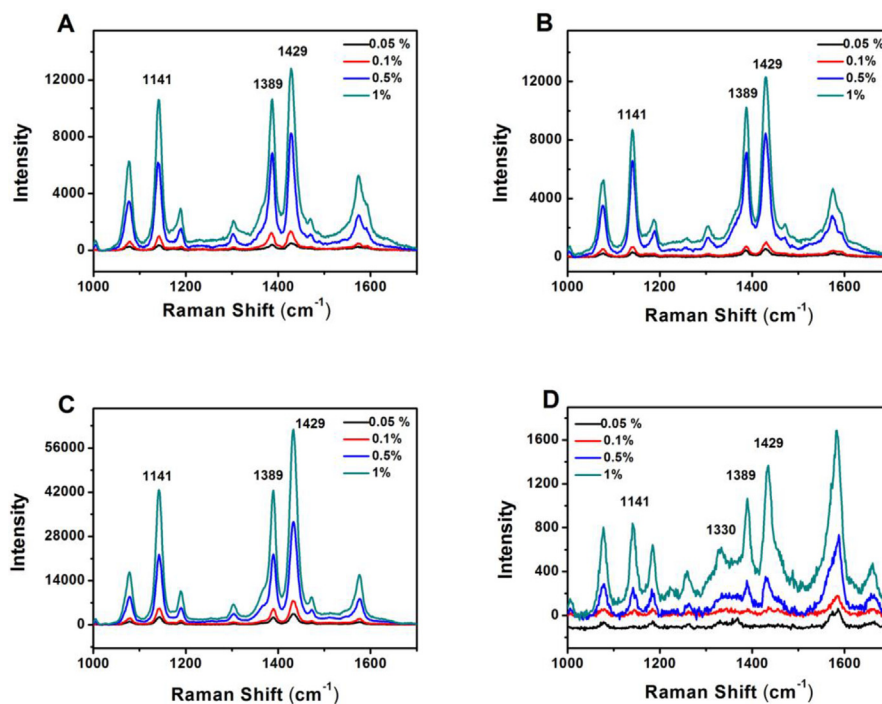


Fig. 3. Power-dependent SERS spectra of PATP in different solutions acquired at an excitation of 532 nm (A) 1,2-butanediol (B) 1,3-butanediol (C) 1,4-butanediol (D) 2,3-butanediol.

Fig. 5 is a mechanistic diagram of the solvent-assisted surface-catalyzed reaction where PATP is dimerized into DMAB under the activity of Ag NPs. It should be noted that, due to the same experimental conditions adopted, the reactive oxygen species owned strong oxidative ability, such as superoxide radicals ($\bullet\text{O}_2^-$) and hydroxyl radicals ($\bullet\text{OH}$), will take crucial role in the titled reactions. However, its effect can be excluded to a certain extent, from the inconsistent enhancement effect of SERS spectrum. That is, the activated oxidation pathway of oxygen does not play a leading role in this catalytic oxidation. Therefore, we believe that the hole-driven oxidation pathway plays a major role in the system studied here. As can be seen that, Ag NPs generate hot electrons due to plasma decay under laser irradiation, which leaves holes [39]. The hot electrons are rapidly captured by the solvent in the system for their own hydroxyl reduction, leaving holes to oxidize the amino group of PATP. However, in the selected butanediol solvent, the ability to capture hot electrons is different due to the different positions of the hydroxyl groups. The hydroxyl group attached to the primary carbon is more likely to collide with the hot electrons due to its position at the end of the molecular structure than the hydroxyl group attached to the secondary carbon, so the rate at which holes remain in the oxidation reaction is also different. That is to say, having two hydroxyl groups attached to the primary carbon makes them more likely to collide with the hot electrons than a single hydroxyl group attached to the primary carbon. Therefore, the rate of capture of hot electrons in the 1,4-butanediol solution is the fastest, leaving more

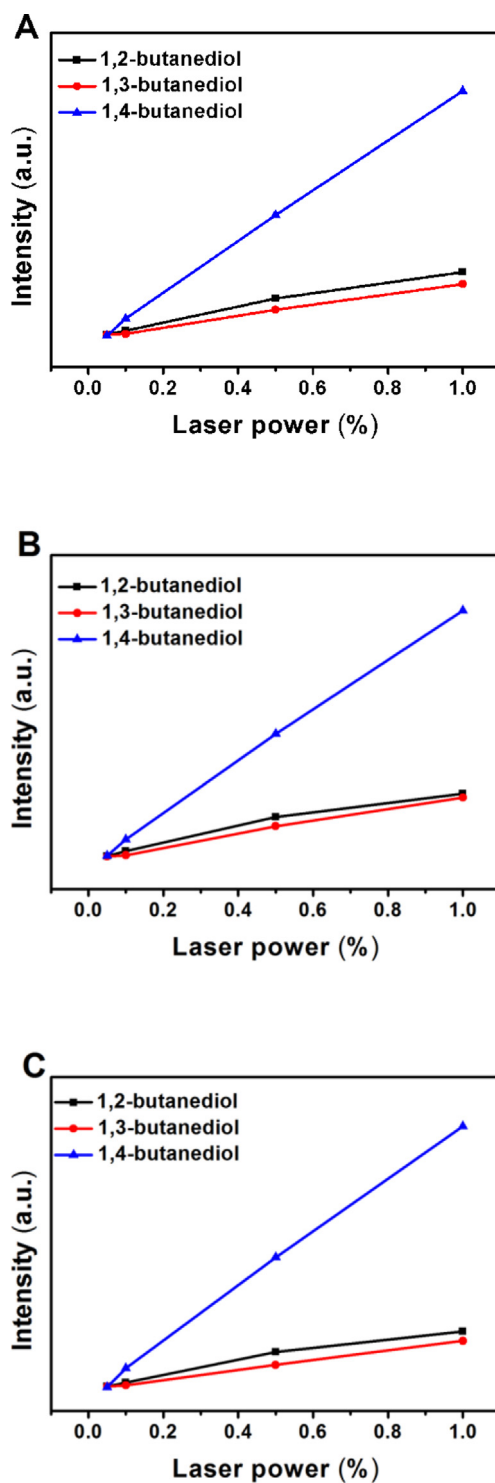


Fig. 4. Power-dependent SERS intensities of DMAB in three different solvents in vibration mode at (A) 1141 cm^{-1} (B) 1389 cm^{-1} , and (C) 1429 cm^{-1} .

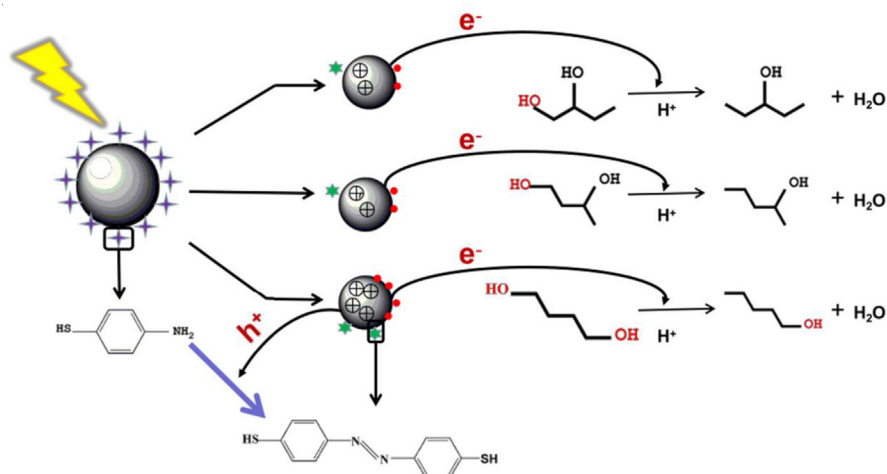


Fig. 5. Diagram of the solvent-assisted surface catalytic reaction mechanisms of PATP dimerization into DMAB under the activity of Ag NPs.

holes to oxidize the PATP and form DMAB. In order to verify our hypothetical mechanism, we conducted the following two sets of experiments.

Fig. 6 shows the power-dependent SERS spectra of PATP in 1,2-propanediol and 1,3-propanediol solvents. It shows that with a low power level of 0.05%, three characteristic peaks of DMAB are generated at 1139, 1389, and 1432 cm^{-1} in both solvents. However, in both solvents, the degree to which the characteristic peaks of DMAB are enhanced varies greatly as the power is increased. It can be seen from the power-dependent SERS spectra that the intensity of the characteristic peak of DMAB in the 1,3-propanediol solution is greater than that in 1,2-propanediol. Combining the experimental results with the molecular structure of the two solvents, it is known that both hydroxyl groups in 1,3-propanediol are attached to the terminal carbon and are more likely to collide with hot electrons to facilitate the reaction.

Fig. 7 shows the power-dependent SERS intensity of DMAB in 1,2-propanediol and 1,3-propanediol. We can clearly observe that the rate of DMAB formation varies greatly between the two solvents. The rate at which PATP dimerizes into DMAB under the action of nanosilver is much faster in 1,3-propanediol than in 1,2-propanediol. This proves our conjecture that the difference in the position of the hydroxyl group in the solvent plays a decisive role in the rate of oxidation reaction. We not only studied the contribution of two propylene glycols to this oxidation reaction, we also selected two pentanediols for verification.

Fig. 8 shows power-dependent SERS spectra of PATP in 1,2-pentanediol and 1,5-pentanediol solvents. Similarly, we can also see from the figure that with a laser irradiation intensity as small as 0.05%, three characteristic peaks of DMAB are generated at 1143, 1389, and 1432 cm^{-1} in both solvents. As the power increases, the enhancement effect of SERS also varies. It can be observed from the SERS spectra

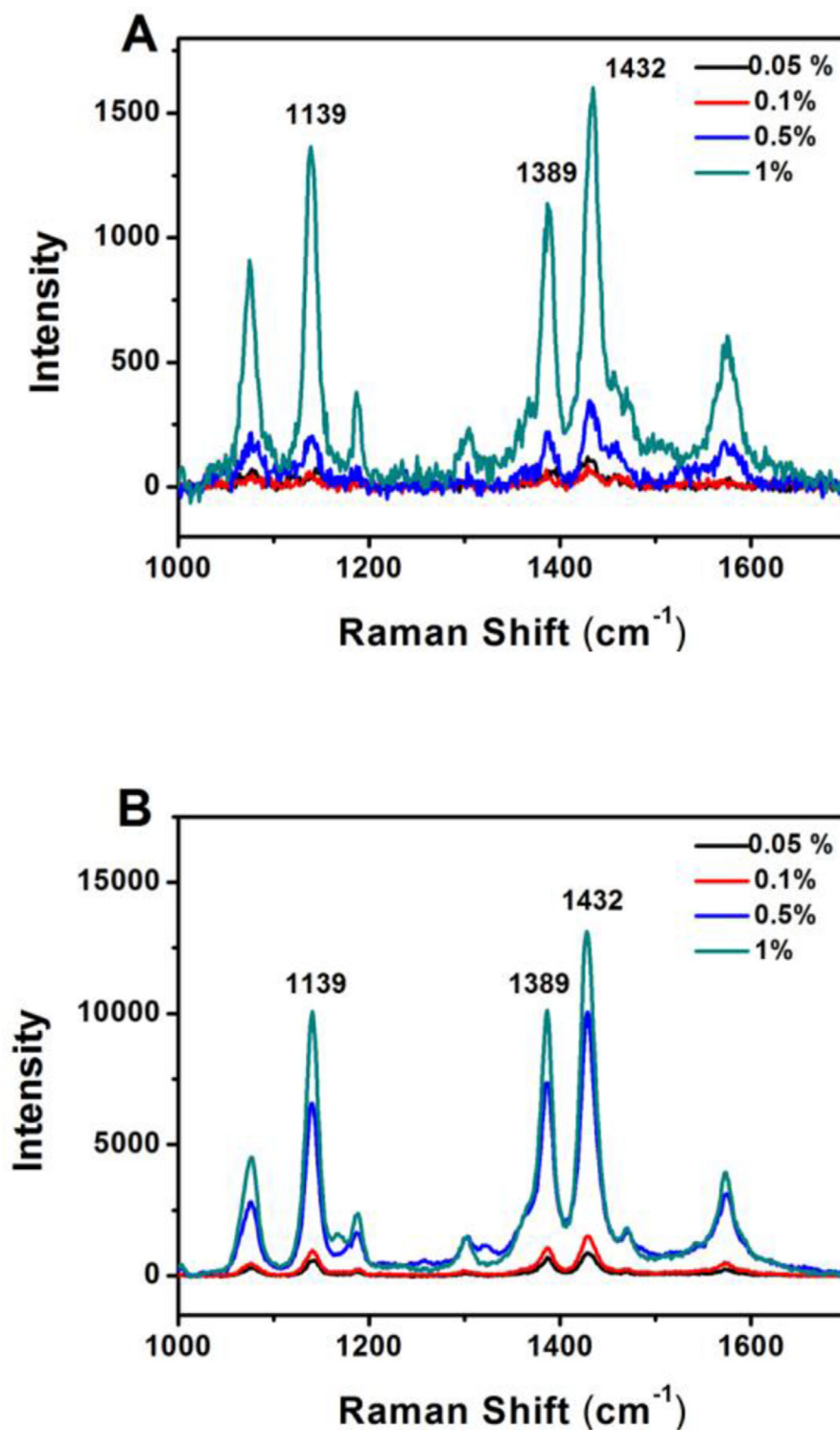


Fig. 6. Power-dependent SERS spectra of PATP in different solutions acquired with an excitation of 532 nm (A) 1,2-propanediol (B) 1,3-propanediol.

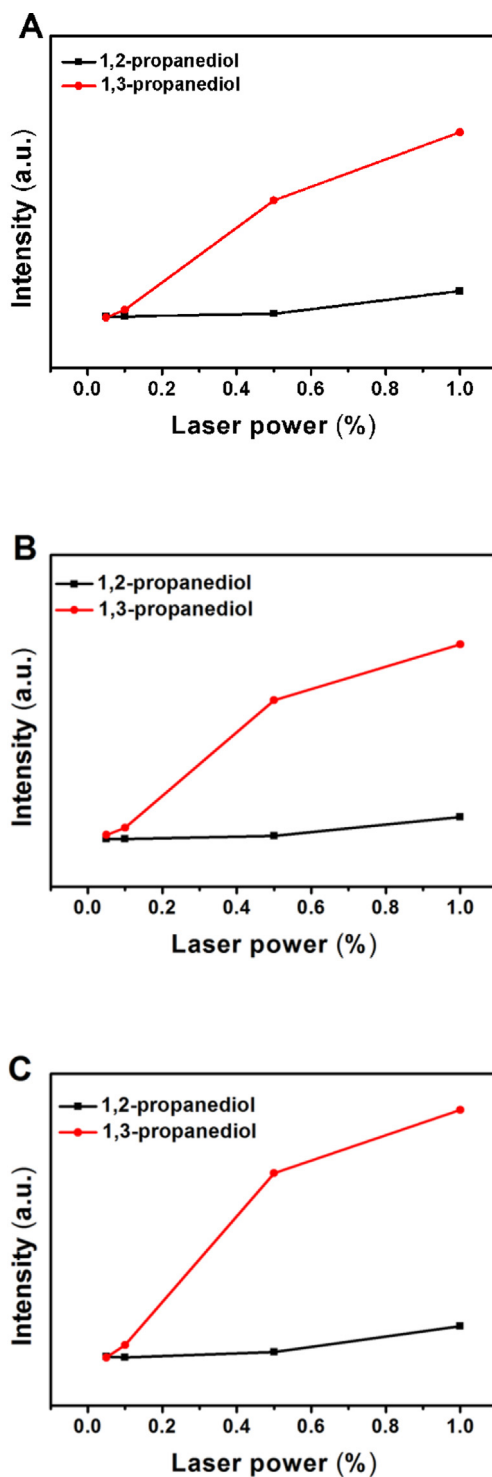


Fig. 7. Power-dependent SERS intensities of DMAB in two different solvents in vibration mode at (A) 1139 cm^{-1} (B) 1389 cm^{-1} and (C) 1432 cm^{-1} .

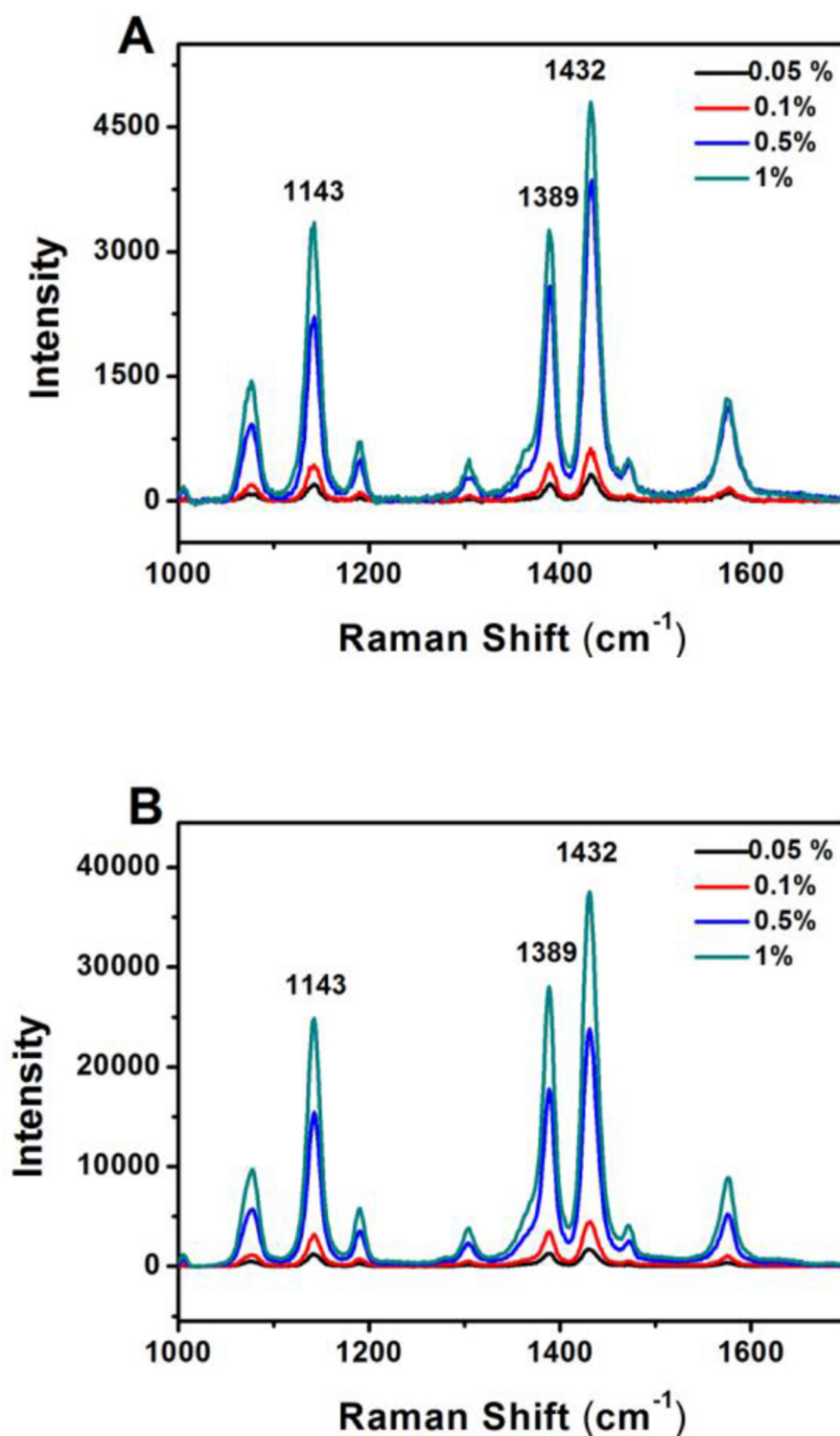


Fig. 8. Power-dependent SERS spectra, acquired with an excitation of 532 nm, of PATP in (A) 1,2-pentanediol; and (B) 1,5-pentanediol.

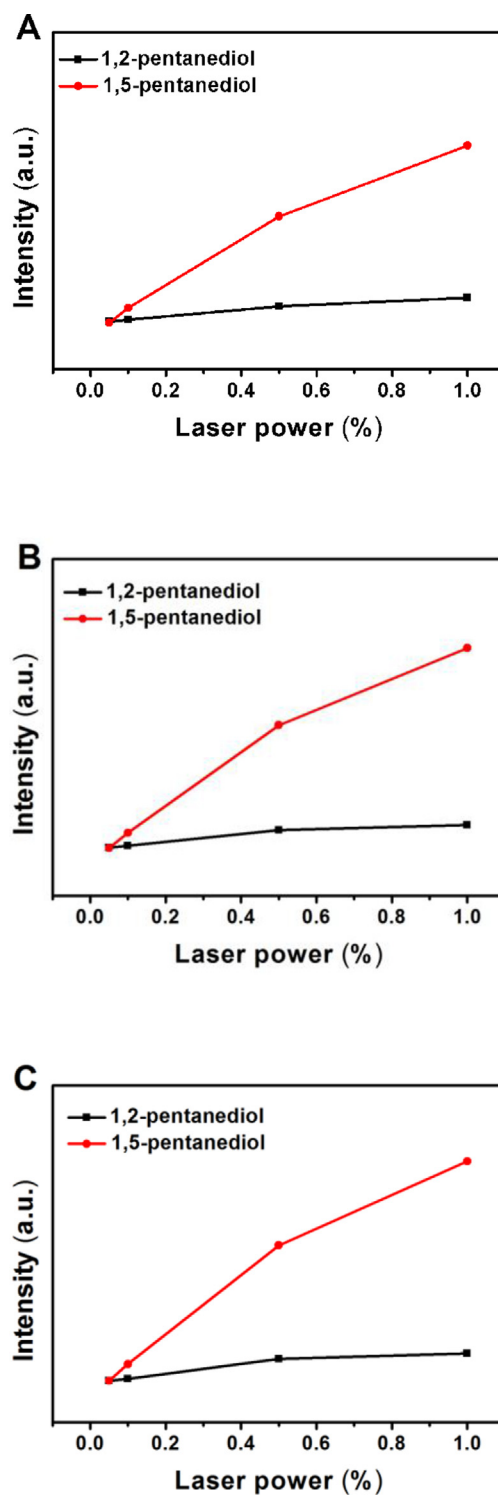


Fig. 9. Power-dependent SERS intensities of DMAB, in two different solvents, in vibration mode at (A) 1143 cm^{-1} (B) 1389 cm^{-1} and (C) 1432 cm^{-1} .

that the absolute intensity of the characteristic DMAB peak differs by ten orders of magnitude in both solvents.

Fig. 9 shows the power-dependent SERS intensity of DMAB in 1,2-pentanediol and 1,5-pentanediol solvents. The three characteristic DMAB peaks are much stronger in the 1,5-pentanediol than in the 1,2-pentanediol. This is also because the two hydroxyl groups in 1,5-pentanediol are located at the end of the carbon chain, which can capture electrons faster and better to promote the surface catalytic oxidation reaction.

4. Conclusions

In this work, we investigated the effect of solvent on the plasma-assisted surface catalytic reaction of PATP being oxidized to DMAB. We selected a variety of diols as reaction solvents, and through a combination of three experiments, we found that the hydroxyl functional groups in the solvent play a regulatory role in the dimerization of PATP into DMAB. From the power-dependent SERS spectra, we can see that the degree to which the intensities of the characteristic DMAB peaks are enhanced varies significantly according to the solvent used. From the power-dependent SERS intensity plots of the three vibration modes of DMAB, we also visually observed that the solvent plays a major role in the reaction rate. Combining the experimental results with structural analysis of the solvent, we found that the terminal hydroxyl functional groups in the solvent are more likely to collide with the hot electrons in the Ag NPs, which accelerates the reaction rate. This study has elucidated the reaction mechanism of PATP dimerization into DMAB, while also determining a simple method by which the reaction rate can be adjusted.

Declarations

Author contribution statement

Peng Song, Lixin Xia: Conceived and designed the experiments; Wrote the paper.

Yu Liu, Dongqi Yang, Yuanchun Zhao: Performed the experiments; Analyzed and interpreted the data; Wrote the paper.

Yanqiu Yang, Shiwei Wu, Jing Wang: Performed the experiments; Analyzed and interpreted the data.

Funding statement

This work was supported by the National Natural Science Foundation of China (21671089 and 21271095), the Scientific Research Fund of Liaoning Province (LT2017010, 20170540409), the Innovative Talent Support Program of Liaoning Province (Grant No. LR2017062), the Liaoning Provincial Department of Education

Project (Grant No. LFW201710), the Shenyang High-level Innovative Talents Program (Grant No. RC180227).

Competing interest statement

The authors declare no conflict of interest.

Additional information

No additional information is available for this paper.

References

- [1] J. Ye, J.A. Hutchison, H. Uji-I, et al., Excitation wavelength dependent surface enhanced Raman scattering of 4-aminothiophenol on gold nanorings, *Nanoscale* 4 (2012) 1606–1611.
- [2] Y.F. Shen, P. Miao, C. Hu, J. Wu, M.S. Gao, P. Xu, SERS-based plasmon-driven reaction and molecule detection on a single Ag@MoS₂ microsphere: effect of thickness and crystallinity of MoS₂, *ChemCatChem* 10 (2018) 3520–3525.
- [3] X.J. Liu, L.H. Tang, R. Niessner, Y.B. Ying, C. Haisch, Nitrite-triggered surface plasmon-assisted catalytic conversion of p-aminothiophenol to p,p'-dimercaptoazobenzene on gold nanoparticle: surface-enhanced Raman scattering investigation and potential for nitrite detection, *Anal. Chem.* 87 (2015) 499–506.
- [4] Y.K. Mishra, R. Adelung, G. Kumar, et al., formation of self-organized silver nanocup-type structures and their plasmonic absorption, *Plasmonics* 8 (2013) 811–815.
- [5] E. Cao, M.T. Sun, Y.Z. Song, W.J. Liang, Exciton-plasmon hybrids for surface catalysis detected by SERS, *Nanotechnology* 29 (2018) 372001.
- [6] B. Ankamwar, U.K. Sur, P. Das, SERS study of bacteria using biosynthesized silver nanoparticles as the SERS substrate, *Anal. Methods* 8 (2016) 2335–2340.
- [7] L.W. Yap, H. Chen, Y. Gao, et al., Bifunctional plasmonic-magnetic particles for an enhanced microfluidic SERS immunoassay, *Nanoscale* 9 (2017) 7822–7829.
- [8] K.M. Tripathi, T.S. Tran, Y.J. Kim, T.Y. Kim, Green fluorescent onion-like carbon nanoparticles from flaxseed oil for visible light induced photocatalytic

- applications and label-free detection of Al(III), *ACS Sustain. Chem. Eng.* 5 (2017) 3982–3992.
- [9] J.M. Romoherrera, A.L. González, L. Guerrini, et al., A study of the depth and size of concave cube Au nanoparticles as highly sensitive SERS probes, *Nano-scale* 8 (2016) 7326–7333.
- [10] W.H. Lin, Y.Q. Cao, P.J. Wang, M.T. Sun, Unified treatment for Plasmon–Exciton Co-driven reduction and oxidation reactions, *Langmuir* 33 (2017) 12102–12107.
- [11] B. Shang, Y.B. Wang, P. Yang, B. Peng, Z.W. Deng, Synthesis of superhydrophobic polydopamine-Ag microbowl/nanoparticle array substrates for highly sensitive, durable and reproducible surface-enhanced Raman scattering detection, *Sensor. Actuator. B Chem.* 255 (2018) 995–1005.
- [12] Y.C. Lai, W.C. Pan, D.J. Zhang, J.H. Zhan, Silver nanoplates prepared by modified galvanic displacement for surface-enhanced Raman spectroscopy, *Nanoscale* 3 (2011) 2134–2137.
- [13] C. Orendorff, L. Gearheart, N. Jana, C. Murphy, Aspect ratio dependence on surface enhanced Raman scattering using silver and gold nanorod substrates, *Phys. Chem. Chem. Phys.* 8 (2006) 165–170.
- [14] S. Watanabe, S. Kaneko, S. Fujii, et al., Gap width-independent spectra in 4-aminothiophenol surface enhanced Raman scattering stimulated in Au-gap array, *J. Appl. Phys.* 56 (2017), 065202.
- [15] X. Ren, E. Cao, W.H. Lin, Y.Z. Song, W.J. Liang, J.G. Wang, Recent advances in surface plasmon-driven catalytic reactions, *RSC Adv.* 7 (2017) 31189–31203.
- [16] X.F. Yan, L.Z. Wang, X.J. Tan, B.Z. Tian, J.L. Zhang, Surface-enhanced Raman spectroscopy assisted by radical capturer for tracking of plasmon-driven redox reaction, *Sci. Rep.* 6 (2016) 30193.
- [17] M.T. Sun, H.X. Xu, A novel application of plasmonics: plasmon-driven surface-catalyzed reactions, *Small* 8 (2012) 2777–2786.
- [18] E. Cao, X. Guo, L.Q. Zhang, et al., Electrooptical synergy on plasmon-exciton-codiven surface reduction reactions, *Adv. Mater. Interfaces* 4 (2017) 1700869.
- [19] L.C. Li, W. Wang, D. Peng, R. Pan, A.M. Tian, Investigation on the photo-driven catalytic coupling reaction mechanism of p-aminothiophenol on the silver cluster, *J. Theor. Comput. Chem.* 14 (2015) 1550019.

- [20] Z.L. Zhang, D. Kinzel, V. Deckert, Photo-Induced or plasmon-induced reaction: investigation of the light-induced azo-coupling of amino groups, *J. Phys. Chem. C* 120 (2016) 20978–20983.
- [21] L. Papa, I. Freitas, R. Geonmonond, et al., Supports matter: unraveling the role of charge transfer in the plasmonic catalytic activity of silver Nanoparticles, *J. Mater. Chem.* 5 (2017) 11720–11729.
- [22] Q. Qiao, C.H. Shan, J. Zheng, et al., Surface plasmon enhanced electrically pumped random lasers, *Nanoscale* 5 (2013) 513–517.
- [23] D.A. Nelson, Z.D. Schultz, Influence of optically rectified electric fields on the plasmonic photocatalysis of 4-nitrothiophenol and 4-aminothiophenol to 4,4-dimercaptoazobenzene, *J. Phys. Chem. C* 122 (2018) 8581–8588.
- [24] H.Y. Wu, Y.H. Lai, M.S. Hsieh, S.D. Lin, Y.C. Li, T.W. Lin, Highly intensified surface enhanced Raman scattering through the formation of p, p'-dimercaptoazobenzene on Ag nanoparticles/graphene oxide nanocomposites, *Adv. Mater. Interfaces* 1 (2014) 1400119.
- [25] E.Z. Tan, P.G. Yin, C.N. Yu, G. Yu, C. Zhao, The oxidant and laser power-dependent plasmon-driven surface photocatalysis reaction of p-aminothiophenol dimerizing into p,p'-dimercaptoazobenzene on Au nanoparticles, *Spectrochim. Acta Mol. Biomol. Spectrosc.* 166 (2016) 15–18.
- [26] Z.L. Zhang, P. Xu, X.Z. Yang, W.J. Liang, M.T. Sun, Surface plasmon-driven photocatalysis in ambient, aqueous and high-vacuum monitored by SERS and TERS, *J Photoch Photobio C* 27 (2016) 100–112.
- [27] B. Dong, Y.R. Fang, X.W. Chen, H.X. Xu, M.T. Sun, Substrate-, wavelength-, and time-dependent plasmon-assisted surface catalysis reaction of 4-nitrobenzenethiol dimerizing to p,p'-dimercaptoazobenzene on Au, Ag, and Cu films, *Langmuir* 27 (2011) 10677–10682.
- [28] W.H. Lin, E. Cao, L.Q. Zhang, et al., Electrically enhanced hot hole driven oxidation catalysis at the interface of a plasmon–exciton hybrid, *Nanoscale* 10 (2018) 5482–5488.
- [29] W.H. Lin, X. Ren, L. Cui, H. Zong, M.T. Sun, Electro-optical tuning plasmon-driven double reduction interface catalysis, *Appl. Mater. Today* 11 (2018) 189–192.
- [30] Z.Y. Zhang, V. Merk, A. Hermanns, W.E.S. Unger, J. Kneipp, Role of metal cations in plasmon-catalyzed oxidation: a case study of p-aminothiophenol dimerization, *ACS Catal.* 7 (2017) 7803–7809.

- [31] Y. Myung, S.H. Jung, T.T. Tung, K.M. Tripathi, T.Y. Kim, Graphene-based aerogels derived from biomass for energy storage and environmental remediation, *ACS Sustain. Chem. Eng.* (2019).
- [32] R.K. Gupta, M. Misra, *Metal Semiconductor Core-Shell Nanostructures for Energy and Environmental Applications*, Elsevier, Netherlands, 2017, pp. 51–78.
- [33] P.C. Lee, D. Meisel, Adsorption and surface-enhanced Raman of dyes on silver and gold sols, *J. Phys. Chem.* 86 (1982) 3391–3395.
- [34] D.Y. Wu, X.M. Liu, Y.F. Huang, B. Ren, X. Xu, Z.Q. Tian, Surface catalytic coupling reaction of p-mercaptoaniline linking to silver nanostructures responsible for abnormal SERS enhancement: a dft study, *J. Phys. Chem. C* 113 (2009) 18212–18222.
- [35] L.X. Xia, C.Q. Ma, J. Wang, S.W. Wu, Y. Liu, Q. Zhang, P. Song, A new strategy for effective distance regulation of the surface plasmon assisted coupling reaction of p-nitrothiophenol to p, p'-dimercaptoazobenzene, *Chem. Commun.* 53 (2017) 9582–9585.
- [36] Y.Z. Huang, Y.R. Fang, Z.L. Yang, M.T. Sun, Can p,p'-dimercaptoazobisbenzene Be produced from p-aminothiophenol by surface photochemistry reaction in the junctions of a Ag nanoparticle-molecule-Ag (or Au) film? *J. Phys. Chem. C* 114 (2010) 18263–18269.
- [37] M.T. Sun, Y.Z. Huang, L.X. Xia, X.W. Chen, H.X. Xu, The pH-controlled plasmon-assisted surface photocatalysis reaction of 4-aminothiophenol to p,p'-dimercaptoazobenzene on Au, Ag, and Cu colloids, *J. Phys. Chem. C* 115 (2011) 9629–9636.
- [38] P. Xu, L.L. Kang, N.H. Mack, K.S. Schanze, X.J. Han, H.L. Wang, Mechanistic understanding of surface plasmon assisted catalysis on a single particle: cyclic redox of 4-aminothiophenol, *Sci. Rep.* 3 (2013) 2997.
- [39] W. Ahn, D.C. Ratchford, P.E. Pehrsson, B.S. Simpkins, Surface plasmon polariton-induced hot carrier generation for photocatalysis, *Nanoscale* 9 (2017) 3010–3022.